

Characterization of Bismuth Titanate by Line Profile Analysis

Dr. Reenu Jacob¹, Ms. Anchana Joseph²

¹CMS College, Kottayam (Autonomous), reenujacob12@gmail.com.

²CMS College, Kottayam (Autonomous), anchana joseph469@gmail.com.

Abstract— Bismuth Titanate (BIT), $\text{Bi}_4\text{Ti}_3\text{O}_{12}$, was synthesized using the solid-state reaction process from the oxide mixture of $\text{Bi}_2\text{O}_3\text{CO}_3$ and TiO_2 . The characterization analysis of the prepared sample was done by X-ray diffraction technique. The X-ray diffraction data revealed an orthorhombic perovskite phase that was clearly explained. The Scherrer method, modified W-H analysis, and the SSP studies were conducted to figure out the crystallite size and micro strain in $\text{Bi}_4\text{Ti}_3\text{O}_{12}$. Morphological studies included SEM and TEM analysis. FTIR spectral investigation supports the M-O coordination of the synthesized $\text{Bi}_4\text{Ti}_3\text{O}_{12}$ sample. The phase formation patterns of $\text{Bi}_4\text{Ti}_3\text{O}_{12}$ determined by different methods are highly connected.

Keywords: BIT ($\text{Bi}_4\text{Ti}_3\text{O}_{12}$), crystallite size, Rietveld refinement, peak indexing.

I. INTRODUCTION

Numerous titanium oxides of the perovskite family exhibit exceptional qualities, allowing for a wide range of applications in several industries. Bismuth Titanate has become a viable material for piezoelectric applications at high temperatures. $\text{Bi}_4\text{Ti}_3\text{O}_{12}$ is a suitable choice for the manufacture of capacitors and memory storage devices due to the presence of high Curie temperature. The high breakdown strength and appreciable dielectric constant of ferroelectric $\text{Bi}_4\text{Ti}_3\text{O}_{12}$ ceramics promote them as a probable staple for device applications.

$\text{Bi}_4\text{Ti}_3\text{O}_{12}$ has orthorhombic symmetry at room temperature. It has three oxygen octahedral bounded by two bismuth oxide layers. The actual symmetry of ferroelectric $\text{Bi}_4\text{Ti}_3\text{O}_{12}$ still encounters diverse opinions as it has been optically defined to be monoclinic but it is determined to be orthorhombic according to diffraction studies. This study has brought up how close optically determined monoclinic angles are to 90° [1–4]. In its paraelectric phase, $\text{Bi}_4\text{Ti}_3\text{O}_{12}$ has a tetragonal crystal structure. According to optical studies, $\text{Bi}_4\text{Ti}_3\text{O}_{12}$ stands different in the Aurivillius family compounds to have a monoclinic ferroelectric structure. Its outstanding and complex electric and piezoelectric effects are due to the resultant complex domain wall structure. Bismuth Titanate in the form of a thin film is highly useful for electro-optic and ferroelectric devices [5].

The broadening of diffraction peaks is evident by diffraction investigations, which demonstrate that divergence from perfect crystallinity develops in all directions [6–8]. The pattern produced by the diffractometer can be used to directly quantify the broadening of X-ray diffraction peaks [9]. Peak width

analysis aids in the extraction of the strain and crystallite size of the sample, which depend on the diffraction order, respectively, and is independent of one another. The development of polycrystalline aggregates made the crystallite size distinct from the particle size [10].

The lattice constants distribution is used to estimate the imperfections of the crystal. Bragg peaks are broadened giving evident changes to the 2θ peak positions [11]. Ungar et.al [12] suggested modifying the W-H method by adding a dislocation contrast factor to consider the anisotropic distribution of dislocation effects on the observed Bragg peaks.

This study covers the characterization of Bismuth Titanate sample produced using a high-energy ball milling procedure. The synthesized sample (Bismuth Titanate) under study was characterized by the XRD technique. The orthorhombic crystalline phase of the synthesized sample was validated by peak indexing and Rietveld refinement method.

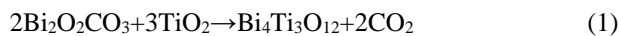
The crystallite size and the peak broadening are measured using the Scherrer method, modified Williamson –Hall plot analysis (UDM, USDM, UDEDM), and the Size-Strain Analysis.

Using UDEDM, the strain (ϵ) as a function of energy density (u) was estimated. The surface morphology of the sample $\text{Bi}_4\text{Ti}_3\text{O}_{12}$ revealed a plate-like structure with a crystallite size of around a few microns.

II EXPERIMENTAL DETAILS

$\text{Bi}_4\text{Ti}_3\text{O}_{12}$ sample under study was synthesized by the solid-state reaction process based on their molecular formula.

For preparing the sample, the reagent-grade chemicals of high purity (99%) TiO₂ and Bi₂O₂CO₃ (rutile crystal form, Carlo Erba p.a 99%) were taken. These raw materials of high purity were weighed based on the molecular formula,



The powders were mixed mechanically in the required stoichiometric ratio. The mechanical mixing was generally carried out by hand mixing in an agate mortar. Then the mixture was ball milled with zirconium balls with a ball speed of 350r/min to assure homogeneity and milling. The mechanically activated process was performed in a planetary ball mill for 0, 60, 120, and 360 min. After the process of milling, the material was calcinated at a very high temperature of 950° C in a furnace. The color of the sample got altered from white to grey at high temperatures.

The XRD measurements explained in this present study are carried out using Bruker AXS D8 Advance X-ray diffractometer with Cu K α ($\lambda= 1.54\text{\AA}$) radiations. The sample is scanned at a pace of 2 degree/minute.

FT-IR spectrum to obtain information for bonding in the sample BIT is recorded in the wave number range from 40-4000cm⁻¹ with a spectral resolution of 0.4cm⁻¹ using Perkin-Elmer Thermo Nicolet, Avatar 370.

The morphology studies of activated powders were obtained from the SEM and TEM analysis(model: JEOL/JEM 2100). TEM image further confirmed its regular sheet-shaped structures.

III. RESULTS

A. LINE PROFILE ANALYSIS

The average size of crystallites in polycrystalline bulk materials is confirmed by employing X-ray diffraction studies [12]. According to crystallographic data, the diffraction peaks of bismuth titanate are totally resolved from one another in the XRD profile of BIT at 950 °C, as shown in Fig. 1. This indicates the production of the orthorhombic perovskite Bi₄Ti₃O₁₂ phase. Scherrer method is used as the widespread technique to obtain the size of the crystallite from the powder diffraction profile. The powder becomes more active as the milling duration is extended.

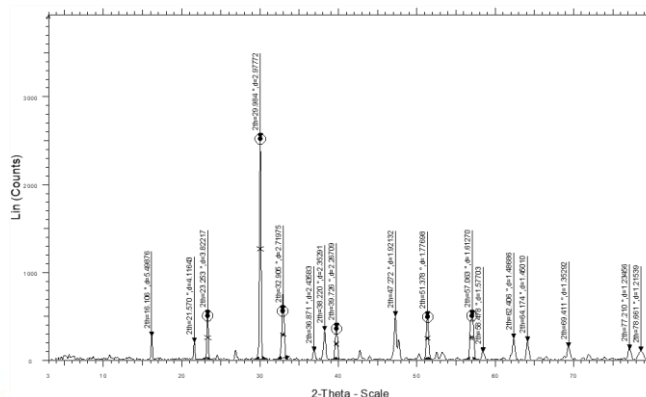


Fig.1: XRD pattern of Bismuth Titanate at 950° C with its peaks detected.

The high-energy ball milling process reduces the size of the sample particles but also induces lattice strain. When the crystallite size is less than 100nm instrumental broadening also affects the width of the peaks. So, the X ray diffraction peaks get broadened instead of giving sharp peaks. The contributions from the instrumental and strain-induced factors to the peak broadening cannot be completely obtained by the Scherrer method. Hence X-ray line profile analysis is generally adopted as it includes all the factors affecting the peak broadening.

The diffraction profile with broadened peaks gives a good chance of micro strain present in the material. FWHM will have low values for sharp peaks and vice versa. The XRD pattern of Bismuth Titanate at 950° C with its peaks detected is given in Fig.1.

The predominant 2 θ values obtained for Bismuth Titanate include 16.106°, 21.570°, 23.253°, 29.994°, and so on. From Fig.1, it can be inferred that corresponding to each 2 θ value, there is a unique FWHM ($\beta(hkl)$) and hence a unique crystallite size depending on the respective peak indices.

The Rietveld refinement using FULLPROF [11] was carried out to refine crystal structure parameters (Fig 2). Rietveld refinement, the characterization technique for crystalline materials makes use of the least square approach to refine the theoretical diffraction profile till it is in agreement with the measured profile. The Rietveld analysis confirms the single-phase orthorhombic structure of BIT.

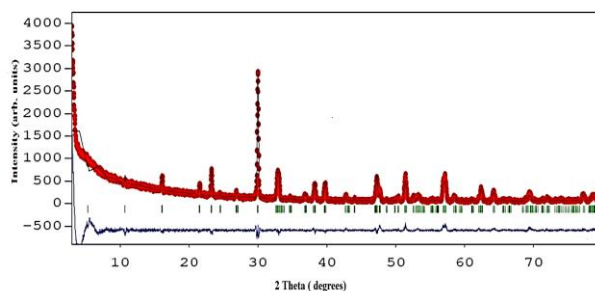


Fig.2: XRD diffraction pattern with Rietveld refinement for Bi₄Ti₃O₁₂ with the orthorhombic structure symmetry.

From the Rietveld analysis, the data obtained as output matched with the standard peak indexing and structural identification parameters of BIT ($\text{Bi}_4\text{Ti}_3\text{O}_{12}$) confirming the sample under study is Bismuth Titanate. The Chi-squared value obtained through Rietveld refinement of the sample is 7.19. The schematic representation of the Aurivillius layered $\text{Bi}_4\text{Ti}_3\text{O}_{12}$ sample is given in Fig.3.

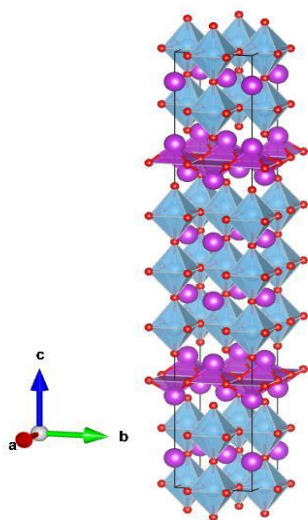


Fig.3. the crystal structure of $\text{Bi}_4\text{Ti}_3\text{O}_{12}$ sample.

B. PEAK INDEXING

The procedure of peak indexing accomplishes peak identification, indexing, and structural identification by comparing the input XRD data with standard crystallographic databases like Crystallographic Open Database (COD). The structure identification data of Bismuth Titanate obtained is given in Table 1.

Table 1: Structure identification data of Bismuth Titanate obtained through peak indexing.

Name	Bismuth Titanate
Formula	$\text{Bi}_4\text{Ti}_3\text{O}_{12}$
Space Group	F m m m
Crystal system	Orthorhombic,
Cell parameters	a=5.4100 Å, b=5.4480 Å c=32.8400 Å
Cell volume	967.92 Å ³
Calc. density	1.8.039 g cm ⁻³

From the peak indexing (COD ID – 1534182), the sample XRD data matched exactly, confirming that the sample is Bismuth titanate with orthorhombic crystal structure and the cell parameters observed are given in Table 2.

Table 2: depicts the atom information of the sample Bismuth Titanate.

Atom	x/a	y/b	z/c	Biso	Occ	Mult
Bi2	.0000	.0000	.2107	.0000	.2500	8
Ti2	.0000	.0000	.3648	.0000	.1250	4
Ti1	.0000	.0000	.5000	.0000	.2500	8
O4	.0000	.0000	.3080	.0000	.2500	8
O1	.2500	.2500	.0000	.0000	.2500	8
O3	.0000	.0000	.4360	.0000	.2500	8
O2	.2500	.2500	.2500	.0000	.2500	8

C. SCHERRER METHOD

The intense reflections X-ray diffraction profile of the sample $\text{Bi}_4\text{Ti}_3\text{O}_{12}$ (BIT) is studied [12] for determining the average of the crystallite size as in equation (2),

$$D = K \lambda / (\beta(hkl) \cos \theta) \quad (2)$$

where D denotes the crystallite size in nm, K is a constant equal to 0.9, λ represents the wavelength of radiation (1.54Å° for Cu K α radiations), $\beta(hkl)$ denotes the peak width at half maximum intensity, and θ is the measured peak position. The results confirm that the crystallite size has value under 100 nm. Average crystallite size(D) of the sample at 950° C obtained is tabulated in Table 3.

Table 3: observed FWHM and crystallite size of Bismuth Titanate calculated using Scherrer formula

Peak position(2 θ)	FWHM (Degree)	Crystallite size(nm)
23.25	0.202	38.52
29.99	0.22	34.88
32.85	0.408	18.67
39.72	0.358	20.87
51.37	0.327	21.89

D. WILLIAMSON – HALL METHODS

If the crystallite size of the polycrystalline material is small [less than 100nm] each behaves as parallel diffracting planes giving broadened diffraction peaks. The instrumental factors also influence peak broadening. The diffraction profile with broadened peaks gives a good chance of strain present in the material. Crystalline samples show sharp peaks in the absence of strain while amorphous samples give humps (diffused halo) in the diffraction profile. The observed peak broadening $\beta(hkl)$ (in radians) in the diffraction profile will be the sum of the broadening due to instrumental factors (β_i) and due to the lattice strain effect broadening (β_r),

$$\beta(hkl) = \beta_i + \beta_r \quad (3)$$

The above equation is true only if the diffracted peak behavior gives a Cauchy profile but when the diffracted peak behavior is partly Cauchy and partly Gaussian, Williamson and Hall proposed the following equation which is more valid as,

$$\beta r = [(\beta(hkl) - \beta_i)(\beta(hkl)) - \beta_i]1/2]1/2 \quad (4)$$

Scherrer equation considers broadening solely due to crystallite size while Williamson-Hall equation reflects the strain induced as well in the material. The lattice strain due to the broadening of the peaks is explained as,

$$\beta r = 4\epsilon \tan \theta \quad (5)$$

where βr is the lattice strain-induced broadening, ϵ the strain distribution within the sample, and ' θ ' the Bragg angle of Xray diffraction. Thus, total broadening $\beta(hkl)$ of diffracted peaks including the lattice strain is explained as,

$$\beta(hkl) = K \frac{\lambda}{D \cos \theta} + 4\epsilon \tan \theta \quad (6) \text{ or}$$

$$\beta(hkl) \cos \theta = K \frac{\lambda}{D} + 4\epsilon \sin \theta \quad (7)$$

The y-intercept obtained from the plot of $(hkl) \cos \theta$ versus $\sin \theta$ specifies crystallite size, while the slope indicates strain induced (ϵ). Fig. 4 depicts the modified W-H plot applying UDM for $\text{Bi}_4\text{Ti}_3\text{O}_{12}$. Crystallite size determined by the Scherrer method is less compared to that from the W-H approach since it does not take into account the strain caused and the instrumental factors present. The X ray diffraction studies of the new material open knowledge into the crystallite size, and the diffraction peaks broaden due to the micro strains and stacking faults within. From Fig 4, the strain observed is positive or the peak shift is to the higher angle side. The ' θ ' shift to the greater angle side confirms a reduction in the lattice constant. The average crystallite size value obtained is less than reported in the literature for pure $\text{Bi}_4\text{Ti}_3\text{O}_{12}$ (~50nm).

1) UDM

In Uniform Deformation Model the strain is assumed to be uniform (isotropic nature of crystal).

On rearranging Eq. (6),

$$\beta(hkl) \cos \theta = \frac{K\lambda}{D} + 4\epsilon \sin \theta \quad (8)$$

Eq. (8) denotes UDM where $\beta(hkl) \cos \theta$ versus $4 \sin \theta$ for the diffraction peaks generated through XRD analysis. The slope and y-intercept of the fitted line provides strain and crystallite size. From the calculations, it is proved that the strain is due to the shrinkage of lattice.

2) USDM

The Uniform Stress Deformation Model (USDM) is plotted on Hook's Law maintaining the linearity between stress and strain present. We assume the crystals to have anisotropic nature.

Hook's law applicable for relatively small values of strain and is given by the equation, $\sigma = Y\epsilon$, where ' σ ' denotes stress, ' Y ' gives Young's modulus and ' ϵ ' denotes the strain [13]. Substituting for $\sigma = Y\epsilon$ gives,

$$\beta(hkl) \cos \theta = \frac{K\lambda}{D} + \frac{4 \sigma \sin \theta}{Y_{hkl}} \quad (9)$$

In USDM plot, $\beta(hkl) \cos \theta$ is plotted against $\frac{4 \sin \theta}{Y_{hkl}}$ assuming standard value for Young's modulus.

The modified W-H plot applying USDM obtained for Bismuth Titanate is shown in Fig. 5. From the results obtained, the stress is calculated from the slope and crystallite size from y-intercept.

3) UDEDM

The energy density (u) of the sample under study is determined using the Uniform Deformation Energy Density Model (UDEDM).

Here the crystal is assumed to be homogeneous and isotropic in all crystallographic orientations. [13]. Hook's Law is employed to calculate the energy density (u), as

$$u = \frac{\epsilon^2 Y_{hkl}}{2} \quad (10)$$

By modifying Eq. (11) considering energy and strain relation as;

$$\beta(hkl) \cos \theta = \frac{K\lambda}{D} + 4 \sin \theta \left(\frac{2u}{Y_{hkl}} \right)^{1/2} \quad (11)$$

For UDEDM Model, $\beta(hkl) \cos \theta$ is plotted against $4 \sin \theta \left(\frac{2u}{Y_{hkl}} \right)^{1/2}$. From the slope obtained, the energy density u can be calculated. The crystallite size is extracted from the y-intercept. As $\sigma = Y\epsilon$, stress ' σ ' can be calculated from energy density ' u ' by the relation $u = \frac{\epsilon^2 Y_{hkl}}{2}$. The modified W-H plot applying UDEDM obtained for Bismuth Titanate (as in Fig. 6). Energy density (u) of the Bismuth Titanate sample calculated from UDEDM is 0.008 J/cm³.

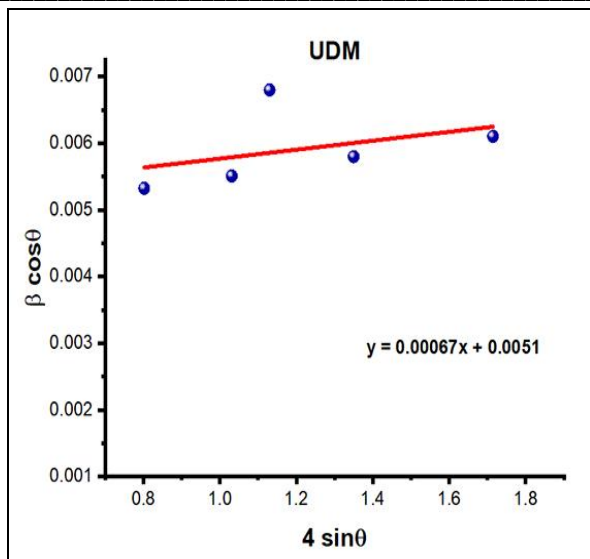


Fig. 4. modified W-H analysis of $\text{Bi}_4\text{Ti}_3\text{O}_{12}$ assuming UDM

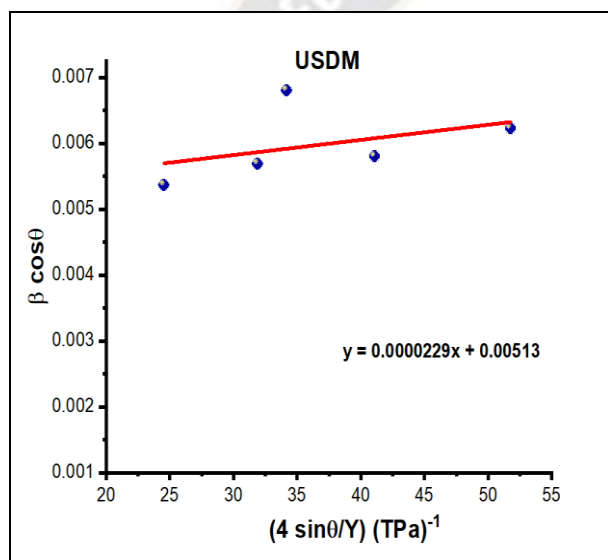


Fig. 5. modified W-H analysis of $\text{Bi}_4\text{Ti}_3\text{O}_{12}$ applying USDM

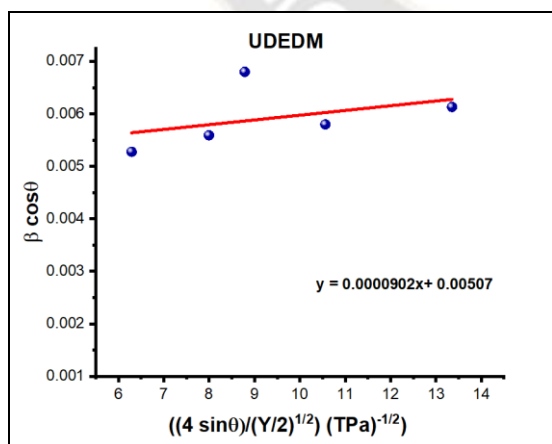


Fig.6: modified W-H analysis of $\text{Bi}_4\text{Ti}_3\text{O}_{12}$ applying UEDM.

IV. SSP METHOD

The crystallite size of sample $\text{Bi}_4\text{Ti}_3\text{O}_{12}$ is calculated by the SSP method as well. Size-strain plots are drawn omitting the high-angle reflections. The Gaussian profile is used for the strain profile whereas the crystallite profile is obtained by the Lorentz function. A graph plotted with $d^2(hkl)\beta(hkl)\cos\theta$ versus $(d(hkl)\beta(hkl)\cos\theta)^2$ gives the size-strain profile of $\text{Bi}_4\text{Ti}_3\text{O}_{12}$ (Fig 7). The strain is obtained from the root of the y-intercept and the crystallite size of the sample under study is calculated from the slope of linearly fitted data.

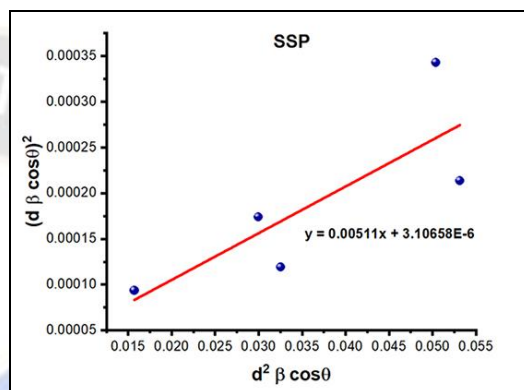


Fig. 7: Size- Strain plot of $\text{Bi}_4\text{Ti}_3\text{O}_{12}$.

Table 4 lists the size and strain of the sample as determined by various analytical methods. All analytical approaches show that the strain obtained is positive or tensile strain.

Table 4: Crystallite size and strain obtained through various analytical methods.

Parameters	Scherrer method	modified W-H plots			Size-strain plot
		UDM	USDM	UEDM	
D(nm)	27	27.18	27.02	27.34	27.13
strain		0.00067	0.00069	0.00070	0.00352

V. FTIR STUDIES OF BISMUTH TITANATE

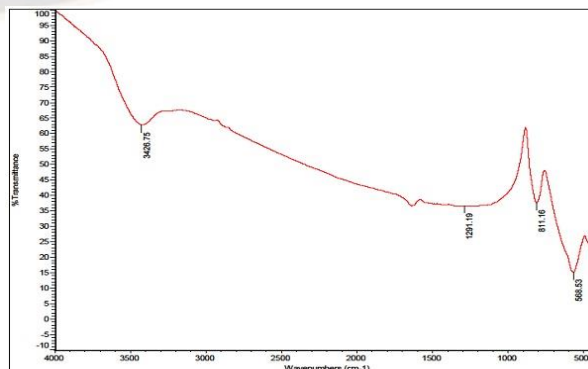


Fig.8: FTIR spectrum of Bismuth Titanate

Fig. 8 depicts the FTIR Spectral patterns for the synthesized $\text{Bi}_4\text{Ti}_3\text{O}_{12}$ sample. Within the specified scan range, FTIR spectra show a molecular vibration bond for stretching vibrations, as well as symmetric and asymmetric stretching conditions ($400\text{-}4000\text{ cm}^{-1}$).

Bi-O bond vibration in synthesized samples is reported to be around 588 cm^{-1} , whilst Ti-O bond linkage is indicated to be around 1000 cm^{-1} [12]. The Ti-O bond is responsible for the stretched band at around 588 cm^{-1} .

VI. MORPHOLOGY STUDIES

The morphological analysis of $\text{Bi}_4\text{Ti}_3\text{O}_{12}$ was carried out using TEM and SEM techniques (model: JEOL/JEM 2100). The crystallite size measurement revealed the plate-like structure of $\text{Bi}_4\text{Ti}_3\text{O}_{12}$ due to its anisotropic nature. Morphology studies reveal that besides plate-like grains, spherical and polygonal grains also exist. The morphologies of the resulting crystallites are $5\mu\text{m}$ wide plate-like shaped and $1\mu\text{m}$ spherical shaped. $\text{Bi}_4\text{Ti}_3\text{O}_{12}$ surface morphology is depicted in Fig. 9. The predominant pyramidal agglomerate shape made the strong powder agglomeration apparent. It is discovered that the results of the TEM and SEM examinations agree with one another.

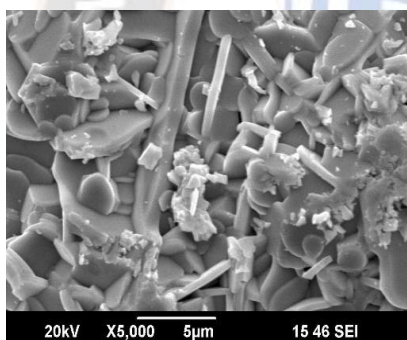


Fig. 9(a)

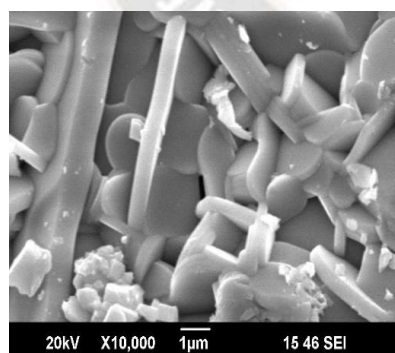


Fig. 9(b)

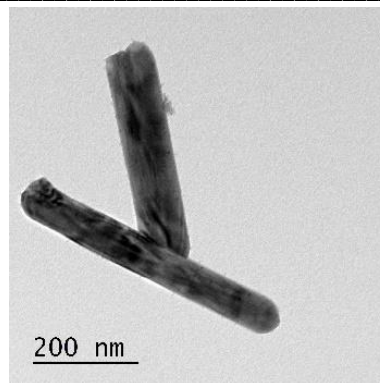


Fig. 9(c)

Figures 9(a), 9(b) & 9(c) depicts the surface morphology images of Bismuth Titanate

VII. CONCLUSION

The structural characterization of the Bismuth Titanate was successfully studied by the X-ray line profile analysis. The Scherrer method, and modified W-H analysis and size-strain method with the positive value of slope obtained points to the presence of tensile strain arising from the defects and interstitials within. The orthorhombic phase of Bismuth Titanate was established by the peak indexing method along with Rietveld refinement technique. Morphological studies from SEM and TEM analysis revealed the plate-like structure of $\text{Bi}_4\text{Ti}_3\text{O}_{12}$ due to its anisotropic nature.

REFERENCES

- [1] H. Hervoches & P. Lightfoot, A Variable-Temperature Powder Neutron Diffraction Study of Ferroelectric $\text{Bi}_4\text{Ti}_3\text{O}_{12}$, *Chem. Mater.*, 11 (1999) 3359. DOI: 10.1002/CHIN.200005005..
- [2] M. Schuisky, CVD and ALD in the Bi-Ti-O System, *Acta Universitatis Upsaliensis*, Uppsala, Sweden (2000). <http://uu.diva-portal.org/smash/get/diva2:166046/FULLTEXT01.pdf>
- [3] H. Buhay et al., Pulsed Laser Deposition (PLD) of Oriented Bismuth Titanate Films for Integrated Electronic Applications, *Appl. Phys. Lett.*, 58 (1991) 1470 <https://doi.org/10.1080/10584589208215713>.
- [4] Prabhu Y Tet. al, X-ray Analysis of Fe doped ZnO Nanoparticles by Williamson-Hall and Size-Strain Plot Methods, *International Journal of Advanced and Engineering Technology* 2(2013)2249–8958. D1393042413/13©BEIESP
- [5] S. Mustapha et al., Comparative study of crystallite size using Williamson-Hall and Debye-Scherrer plots for ZnO nanoparticles, *Advances in Natural Sciences: Nanoscience and Nanotechnology*, 10 (2019) Article ID 045013. DOI 10.1088/2043-6254/ab52f7
- [6] VD Mote et al, Williamson-Hall analysis in estimation of lattice strain in nanometer-sized ZnO particles, *Journal of Theoretical and Applied Physics* 6:6 (2012), <http://www.jtaphys.com/content/2251-7235/6/1/6>
- [7] K. Ramakanth, *Basic of Diffraction and Its Application*, I.K. International Publishing House Pvt. Ltd, New Delhi (2007). ISBN 13 9789381141540W. D. Doyle, "Magnetization reversal

- in films with biaxial anisotropy,” in 1987 Proc. INTERMAG Conf., pp. 2.2-1–2.2-6.
- [8] GK Williamson, W H Hall, Effect of Nitriding Current Density on the Surface Properties and Crystallite Size of Pulsed Plasma-Nitrided AISI 316L, *Acta Metall. Mater*,1(1953)22. DOI:[10.4236/msce.2015.31007J](https://doi.org/10.4236/msce.2015.31007J). Williams, “Narrow-band analyzer (Thesis or Dissertation style),” Ph.D. dissertation, Dept. Elect. Eng., Harvard Univ., Cambridge, MA, 1993.
- [9] T Ungar, T Trichy, The Effect of Dislocation Contrast on X-Ray Line Profiles in Untextured Polycrystals, *IPSSA* (1999),425-434. DOI:[10.1002/\(SICI\)1521-396X\(199902\)171:2<425::AID-PSSA425>3.0.CO;2-W](https://doi.org/10.1002/(SICI)1521-396X(199902)171:2<425::AID-PSSA425>3.0.CO;2-W)
- [10] Lingli Wanga et al., Bi 4 Ti 3 O 12 Synthesized by High Temperature Solid Phase Method and it's Visible Catalytic Activity, *Procedia Environmental Sciences* 18 (2013) 547 – 558. doi: 10.1016/j.proenv.2013.04.074.
- [11] J. Rodríguez-Carvajal & T. Roisnel, FullProf, WinPLOTR and accompanying programs at <http://www-llb.cea.fr/fullweb/powder.htm>. (1999).
- [12] K. Maniammal, G. Madhu, V. Biju, X-ray diffraction line profile analysis of nanostructured nickel oxide: Shape factor and convolution of crystallite size and micro strain, *Physica E* 85(2017)214-222. <https://doi.org/10.1016/j.physe.2016.08.035>.
- [13] V. Biju et al., A Comparative Study on the Milling Speed for the Synthesis of Nano-Structured Al 6063 Alloy Powder by Mechanical Alloying *Journal of Materials Science*, 43 (2008)1175–1179. <https://doi.org/10.1007/s10853-007-2300-8>.

